

Published in final edited form as:

*Neurosci Lett.* 2011 November 7; 505(1): 19–24. doi:10.1016/j.neulet.2011.09.040.

## Breaches of the pial basement membrane are associated with defective dentate gyrus development in mouse models of congenital muscular dystrophies

Jing Li<sup>1</sup>, Miao Yu<sup>1</sup>, Gang Feng<sup>2</sup>, Huaiyu Hu<sup>1</sup>, and Xiaofeng Li<sup>2</sup>

<sup>1</sup>Department of Neuroscience and Physiology, SUNY Upstate Medical University, Syracuse, NY 13210, USA.

<sup>2</sup>Department of Neurology, the Second Affiliated Hospital of Chongqing Medical University, Chongqing, PRC.

### Abstract

A subset of congenital muscular dystrophies (CMDs) has central nervous system manifestations. There are good mouse models for these CMDs that include *POMGnT1* knockout, *POMT2* knockout and Large<sup>myd</sup> mice with all exhibit defects in dentate gyrus. It is not known how the abnormal dentate gyrus is formed during development. In this study, we conducted a detailed morphological examination of the dentate gyrus in adult and newborn *POMGnT1* knockout, *POMT2* knockout, and Large<sup>myd</sup> mice by immunofluorescence staining and electron microscopic analyses. We observed that the pial basement membrane overlying the dentate gyrus was disrupted and there was ectopia of granule cell precursors through the breached pial basement membrane. Besides these, the knockout dentate gyrus exhibited reactive gliosis in these mouse models. Thus, breaches in the pial basement membrane are associated with defective dentate gyrus development in mouse models of congenital muscular dystrophies.

### Keywords

Congenital muscular dystrophies; dentate gyrus; brain development; basement membrane

### Introduction

Congenital muscular dystrophies (CMDs) with central nervous system manifestations are a group of heterogeneous genetic diseases, including Fukuyama congenital muscular dystrophy (FCMD), muscle-eye-brain disease (MEB), Walker-Warburg syndrome (WWS), and congenital muscular dystrophy 1D (CMD1D) [1-8]. Their mutated genes are *FKTN* (encoding fukutin), *POMGnT1* (encoding protein O-mannose N-acetylglucosaminyltransferase 1, POMGnT1), *POMT1* (encoding protein O-mannosyltransferase 1, POMT1), *POMT2* (encoding POMT2), and *LARGE*, (encoding like-glycosyltransferase, LARGE), [9-17], respectively. All of these proteins contain

© 2011 Elsevier Ireland Ltd. All rights reserved.

Address correspondence to: Xiaofeng Li Department of Neurology The Second Affiliated Hospital of Chongqing Medical University Chongqing, PRC lixfq@yahoo.com.cn.

**Publisher's Disclaimer:** This is a PDF file of an unedited manuscript that has been accepted for publication. As a service to our customers we are providing this early version of the manuscript. The manuscript will undergo copyediting, typesetting, and review of the resulting proof before it is published in its final citable form. Please note that during the production process errors may be discovered which could affect the content, and all legal disclaimers that apply to the journal pertain.

glycosyltransferase domains. The main implicated structures of the central nervous system include the cerebrum, the cerebellum, and the pons; manifesting micropolygyria, hypoplasia of the pons, and hydrocephalus. Mental retardation is one of the prominent symptoms [11].

Dentate gyrus, which is one of the components of the hippocampus formation, plays a critical role in processing memory and learning. In mouse models of CMD, *POMGnT1* knockout mice [12], brain-specific knockout mice of *POMT2* [18] and *Large<sup>myd</sup>* mice [14] exhibit abnormal dentate gyrus morphologies. However, no further investigation concerning this has been performed and it is still unknown how the abnormal dentate gyrus is formed during development. In this study, detailed morphological investigation of the dentate gyrus of adult and newborn mice was performed in *POMGnT1* knockout mice, *POMT2* knockout mice, and *Large<sup>myd</sup>* mice.

## Materials and Methods

### Animals

*POMGnT1* knockout mice were generated in collaboration with Lexicon Genetics [12]. *POMT2*-floxed mice were generated at the Transgenic and Knockout Mouse Facility at the University of Connecticut Health Sciences Center [13]. *Large<sup>myd</sup>* and *Emx1-Cre* knock-in mice were obtained from the Jackson Laboratories (Bar Harbor, ME). Adult (> 2 months old) and newborn (postnatal day 3) homozygous mice were used in the study. Littermate wild-types (+/+) were used as controls. Animal care and usage were approved by the Institutional Animal Care and Use Committee of SUNY Upstate Medical University and adhered to the the guidelines of the National Institutes of Health.

### Immunofluorescence staining

Antibodies were obtained as follows: Rabbit poly clonal anti-laminin and anti-GFAP (used at 1:1000 dilutions) from Sigma-Aldrich (St. Louis, MO). Polyclonal anti-Prox1 (used at 1:500 dilutions) from Abcam (Cambridge, MA). Anti-rabbit IgG antibody produced in goat conjugated with Rhodamine and anti-rabbit IgG antibody produced in goat conjugated with FITC (used at 1:500 dilutions) from Vector Laboratories (Burlingame, USA).

Mice were anesthetized and decapitated. Whole brain was removed from the skull and the forebrain was dissected and embedded in optimal cutting temperature (OCT) compound in cryomolds and frozen in dry ice/2-methylbutane bath. The frozen tissues were cut into 10  $\mu\text{m}$  sections in a coronal plane and mounted on Superfrost plus slides (Fisher Scientific, Pittsburgh, PA). After the sections were air-dried, they were fixed with 4% paraformaldehyde for 15 minutes. To stain with antibodies, the sections were incubated with 3.0% bovine serum albumin in Tris-buffered saline (TBS, 50 mM Tris, pH7.4, 150 mM NaCl) to block non-specific binding. The sections were then incubated with the indicated primary antibody overnight at 4°C. After washing with TBS containing 0.1% Triton X-100, the sections were incubated with FITC-conjugated goat anti-mouse IgG or anti-rabbit IgG for 2 hours. After washing, all sections were counterstained for 10 minutes with 0.10% DAPI (Sigma-Aldrich, St. Louis, MO) before being mounted with coverslips. Fluorescence was visualized with a Zeiss Axioskop upright fluorescence microscope equipped with a digital camera (Carl Zeiss Microimaging, Inc., Thornwood, NY).

### Electron microscopic analysis

Electron microscopic analysis of the dentate gyrus was carried out essentially as previously described [19]. The samples were observed, and photographs were taken with a Tecnai T12 transmission electron microscope (FEI Company, Salem, MA).

## Results

### Disruptions of the pial basement membrane at the dentate gyrus in CMD mouse models

To examine the integrity of the pial basement membrane in the dentate gyrus of *POMGnT1* knockout mice and other available mouse models of CMDs, we carried out laminin immunofluorescence staining on sections of adult brains (Figure 1). In the wildtype, there were two lines of immunofluorescence separating the dentate gyrus and the midbrain, one representing the pial basement membrane of the hippocampus (arrows in Figure 1A) and the other representing the pial basement membrane of the midbrain (arrowheads in Figure 1A). In *POMGnT1* knockout (Figure 1B), disruptions of the pial basement membrane were apparent in addition to the characteristic architectural abnormality of the inferior blade (Figure 1B). In some areas, only a single pial basement membrane (belonging to the midbrain, arrowhead in Figure 1B) was seen. In other areas, pial basement membrane was absent (asterisks in Figure 1B). Similar results were obtained for *POMT2<sup>f/f</sup>;Emx1-Cre* mice (Figure 1C), where only the pial basement membrane of the midbrain remained in an area with apparent dysmorphological appearance of the inferior blade and the pial basement membrane of the dentate gyrus was absent. Also, similar results were obtained for *Large<sup>myd</sup>* mice (Figure 1D). These results suggest that the pial basement membrane overlying the dentate gyrus was disrupted in these mouse models of CMDs.

### EM analysis confirmed pial basement membrane disruptions at the dentate gyrus

To confirm that the pial basement membrane of the dentate gyrus in the mouse models of CMDs was defective, we performed electron microscopic analysis. In the wildtype (Figure 2A), two basement membranes were identified at the border of the dentate gyrus and the midbrain. One of the basement membranes belonged to the dentate gyrus (arrows in Figure 2A); the other to the midbrain (arrowheads in Figure 2A). Between the two pial basement membranes, fibroblasts of the pial mater were identified. Blood vessels were also occasionally observed between the two pial basement membranes (not shown). In *POMGnT1* knockout mice, basement membrane was sometimes completely missing (Figure 2B). In *POMT2<sup>f/f</sup>;Emx1-Cre(+)* mice, there was only a single basement membrane at the border of the dentate gyrus and the midbrain (arrowheads in Figure 2C). Similar results were obtained from *Large<sup>myd</sup>* mice (Figure 2D). These results indicate that the pial basement membrane is disrupted between the dentate gyrus and the midbrain in the mouse models of CMDs.

### Reactive gliosis at the dentate gyrus

The neocortex of *POMGnT1* knockout mice exhibited extensive reactive gliosis[26]. To examine whether reactive gliosis existed in the dentate gyrus of the mouse models of congenital muscular dystrophy, we carried out immunofluorescence staining with an antibody against GFAP (Figure 3). In the wildtype, GFAP-positive astrocytes were sporadically distributed across the dentate gyrus. Two GFAP-labeled glia limitans were observed at the border between the dentate gyrus and the midbrain (arrows in Figure 3A). In *POMGnT1* knockout mice, GFAP-positive astrocytes were increased in number with apparently increased fluorescence intensity. Glia limitans was observed but disrupted because it was discontinuous (arrows in Figure 3B). An increase in GFAP-positive cells was observed only at the lower blade of the dentate gyrus. Similarly, an increased number of GFAP-positive astrocytes at the lower blade of the dentate gyrus were also found in *POMT2<sup>f/f</sup>;Emx1-Cre(+)* and *Large<sup>myd</sup>* mice (Figure 3C and D, respectively).

## Ectopia of granule cell precursors through the breached pial basement membrane during development

To determine the relationship between the disruptions of the pial basement membrane and the granule precursors of the dentate gyrus, we examined the pial basement membrane of newborn mice. Newborn forebrain sections were double stained with antibodies against laminin-1 and Prox1 (a marker for dentate gyrus granule cell precursors) (Figure 4). In the wildtype, laminin immunofluorescence revealed two lines of staining (red fluorescence) at the border of the developing dentate gyrus and the midbrain representing two pial basement membranes, one for the dentate gyrus, and the other for the midbrain. Prox1-positive granule cell precursors were observed at the developing blades of the dentate gyrus. The closest nuclei of Prox1-positive neurons to the pial basement membrane were separated from the pial basement membrane by about 50  $\mu\text{m}$ . In *POMGnT1* knockout mice, we discerned only one continuous line of laminin immunofluorescence staining (and sometimes none) representing the pial basement membrane of the midbrain. Some Prox1-positive nuclei were apparently mislocalized at positions very close to the pial basement membrane (square in Figure 4B). In *POMT2<sup>f/f</sup>;Emx1-Cre* knockout mice, the pial basement membrane of the dentate gyrus also disappeared (Figure 4C). A number of Prox1-positive nuclei were ectopic and some of these neurons were located very close to the pial basement membrane of the midbrain (square in Figure 4C). Similar results were also observed for *Large<sup>myd</sup>* mice (Figure 4D). Complete absence of pial basement membrane was observed in some areas (asterisks in Figure 4D). Again, some Prox1-positive nuclei were very closely positioned to the pial basement membrane. These results indicate that the pial basement membrane of the dentate gyrus (and sometimes the midbrain) is disrupted and that some granule precursors are ectopically located.

## Discussion

Dentate gyrus abnormalities in *POMGnT1* knockout [12], *POMT2* knockout [18], and *Large<sup>myd</sup>* mice [14] include a wavy morphology of the inferior blade (endal blade). In this study, we showed that this dysmorphology is composed of disruptions of the pial basement membrane and ectopia of dentate gyrus. Such disruptions were present during postnatal development, which is associated with ectopia of granule cell precursors.

CMDs with central nervous system manifestations are termed as alpha - dystroglycanopathies, for of which all the mutated genes encode glycosyltransferases, participating in the process of glycosylation of  $\alpha$ -dystroglycan ( $\alpha$ -DG). Mutations in these (presumed) glycosyltransferases cause hypoglycosylation of  $\alpha$ -DG [12] [20-25], which is the fundamental cause of common manifestations, including muscular dystrophy, ophthalmic malformation, and brain dysfunction.  $\alpha$ -DG is a cell surface receptor for extracellular matrix proteins, such as laminin [26-30][20], agrin [31;32], perlecan [33;34] and pikachurin [35]. Hypoglycosylation of  $\alpha$ -DG in CMDs results in diminished interactions with the extracellular matrix molecules, which are integral components of the basement membrane, a proteinaceous membrane covering the entire central nervous system and separating the neural tissue from the overlying mesenchymal pia mater. In our present study, laminin immunofluorescence staining on sections of adult brains showed disruptions of the pial basement membrane at the dentate gyrus, which was confirmed by EM. Hypoglycosylation of  $\alpha$ -DG may underlie the breaches of the pial basement membrane, which may be the key initial event [24].

Besides the breaches of the pial basement membrane, we also observed ectopia of the inferior blade of the dentate gyrus in CMD mouse models. The disruptions of pial basement membrane and the ectopia of the inferior blade of the dentate gyrus seemed highly correlated. In our previous studies, we have shown that pial basement membrane disruptions

in two other brain regions in congenital muscular dystrophies: the neocortex [24] and the cerebellum [25]. During development of the neocortex of *POMGnT1* knockout mice, breaches in the pial basement membrane result in emigration of many neurons into the pia-arachnoid space [36]. During development of the knockout cerebellum, the pial basement membrane disappears in localized areas, resulting in ectopias of external germinal layer precursors through these breaches. The ectopic neurons failed to migrate to the granule cell layer [25]. Disruptions of the pial basement membrane underlie overmigration of neurons in the neocortex and migration failure of granule cells in the cerebellum of *POMGnT1* knockout mice. Thus, the seemingly different migration defects in the neocortex (overmigration) and the cerebellum (migration failure) are caused by similar cellular pathomechanisms; i.e., the disruptions in the basement membrane resulting in neuronal ectopia beyond the neural boundary. We therefore speculated that disruptions in the pial basement membrane also result in abnormal migration of dentate granule precursors which precede the formation of the abnormal dentate morphology. In our experiment, in the inferior blade of the dentate gyrus in newborn *POMGnT1* knockout, brain-specific knockout of *POMT2*, and *Large<sup>myd</sup>* mice, ectopia of prox1-positive granule neuron precursors exist near the broken pial basement membrane, which is consistent with our speculation.

In the GFAP immunofluorescence staining, we observed that the inferior blade of the *POMGnT1* knockout, brain-specific knockout of *POMT2*, and *Large<sup>myd</sup>* mice exhibited increased expression of GFAP by the astrocytes, indicative of reactive astrogliosis. This phenomenon has been observed in the neocortex of *POMGnT1* knockout mice [37]. Reactive gliosis also exists in the neocortex of brain-specific knockout of *POMT2* and the *Large<sup>myd</sup>* mice (unpublished results). Since reactive astrocytes are associated with various pathological changes in the brain, the roles of reactive astrocytes in brain malfunction of CMD patients will need to be evaluated.

## Acknowledgments

This work was supported by grants from the National Institutes of Health HD060458 and NS066582 (to H.H) and a grant from the National Natural Science Funds of China No.30800346 (to X.L).

## References

- [1]. Haltia M, Leivo I, Somer H, Pihko H, Paetau A, Kivela T, Tarkkanen A, Tome F, Engvall E, Santavuori P. Muscle-eye-brain disease: a neuropathological study. *Ann. Neurol.* 1997; 41:173–180. [PubMed: 9029066]
- [2]. van der Knaap MS, Smit LM, Barth PG, Catsman-Berrepoets CE, Brouwer OF, Begeer JH, de C, Valk I,J. Magnetic resonance imaging in classification of congenital muscular dystrophies with brain abnormalities. *Ann. Neurol.* 1997; 42:50–59. [PubMed: 9225685]
- [3]. Lian G, Sheen V. Cerebral developmental disorders. *Curr. Opin. Pediatr.* 2006; 18:614–620. [PubMed: 17099359]
- [4]. Dobyns WB, Kirkpatrick JB, Hittner HM, Roberts RM, Kretzer FL. Syndromes with lissencephaly. II: Walker-Warburg and cerebro-oculo-muscular syndromes and a new syndrome with type II lissencephaly. *Am. J. Med. Genet.* 1985; 22:157–195. [PubMed: 3931474]
- [5]. Ross ME, Walsh CA. Human brain malformations and their lessons for neuronal migration. *Annu. Rev. Neurosci.* 2001; 24:1041–1070. [PubMed: 11520927]
- [6]. Parano E, Pavone L, Fiumara A, Falsaperla R, Trifiletti RR, Dobyns WB. Congenital muscular dystrophies: clinical review and proposed classification. *Pediatr. Neurol.* 1995; 13:97–103. [PubMed: 8534290]
- [7]. Jimenez-Mallebrera C, Brown SC, Sewry CA, Muntoni F. Congenital muscular dystrophy: molecular and cellular aspects. *Cell Mol. Life Sci.* 2005; 62:809–823. [PubMed: 15868406]
- [8]. Golden JA. Cell migration and cerebral cortical development. *Neuropathol. Appl. Neurobiol.* 2001; 27:22–28. [PubMed: 11298998]

- [9]. Beltran-Valero de BD, Currier S, Steinbrecher A, Celli J, van BE, van der ZB, Kayserili H, Merlini L, Chitayat D, Dobyns WB, Cormand B, Lehesjoki AE, Cruces J, Voit T, Walsh CA, van BH, Brunner HG. Mutations in the O-mannosyltransferase gene POMT1 give rise to the severe neuronal migration disorder Walker-Warburg syndrome. *Am. J. Hum. Genet.* 2002; 71:1033–1043. [PubMed: 12369018]
- [10]. van Reeuwijk J, Janssen M, van den Elzen C, Beltran-Valero de BD, Sabatelli P, Merlini L, Boon M, Scheffer H, Brockington M, Muntoni F, Huynen MA, Verrips A, Walsh CA, Barth PG, Brunner HG, van Bokhoven H. POMT2 mutations cause alpha-dystroglycan hypoglycosylation and Walker-Warburg syndrome. *J. Med. Genet.* 2005; 42:907–912. [PubMed: 15894594]
- [11]. Yoshida A, Kobayashi K, Manya H, Taniguchi K, Kano H, Mizuno M, Inazu T, Mitsuhashi H, Takahashi S, Takeuchi M, Herrmann R, Straub V, Talim B, Voit T, Topaloglu H, Toda T, Endo T. Muscular dystrophy and neuronal migration disorder caused by mutations in a POMGnT1, glycosyltransferase. *Dev. Cell.* 2001; 1:717–724. [PubMed: 11709191]
- [12]. Kobayashi K, Nakahori Y, Miyake M, Matsumura K, Kondo-Iida E, Nomura Y, Segawa M, Yoshioka M, Saito K, Osawa M, Hamano K, Sakakihara Y, Nonaka I, Nakagome Y, Kanazawa I, Nakamura Y, Tokunaga K, Toda T. An ancient retrotransposal insertion causes Fukuyama-type congenital muscular dystrophy. *Nature.* 1998; 394:388–392. [PubMed: 9690476]
- [13]. Longman C, Brockington M, Torelli S, Jimenez-Mallebrera C, Kennedy C, Khalil N, Feng L, Saran RK, Voit T, Merlini L, Sewry CA, Brown SC, Muntoni F. Mutations in the human LARGE gene cause MDC1D, a novel form of congenital muscular dystrophy with severe mental retardation and abnormal glycosylation of alpha-dystroglycan. *Hum. Mol. Genet.* 2003; 12:2853–2861. [PubMed: 12966029]
- [14]. Currier SC, Lee CK, Chang BS, Bodell AL, Pai GS, Job L, Lagae LG, Al-Gazali LI, Eyaid WM, Enns G, Dobyns WB, Walsh CA. Mutations in POMT1 are found in a minority of patients with Walker-Warburg syndrome. *Am. J. Med. Genet. A.* 2005; 133:53–57. [PubMed: 15637732]
- [15]. de Bernabe DB, van BH, van BE, Van den AW, Kant S, Dobyns WB, Cormand B, Currier S, Hamel B, Talim B, Topaloglu H, Brunner HG. A homozygous nonsense mutation in the fukutin gene causes a Walker-Warburg syndrome phenotype. *J. Med. Genet.* 2003; 40:845–848. [PubMed: 14627679]
- [16]. Brockington M, Yuva Y, Prandini P, Brown SC, Torelli S, Benson MA, Herrmann R, Anderson LV, Bashir R, Burgunder JM, Fallet S, Romero N, Fardeau M, Straub V, Storey G, Pollitt C, Richard I, Sewry CA, Bushby K, Voit T, Blake DJ, Muntoni F. Mutations in the fukutin-related protein gene (FKRP) identify limb girdle muscular dystrophy 2I as a milder allelic variant of congenital muscular dystrophy MDC1C. *Hum. Mol. Genet.* 2001; 10:2851–2859. [PubMed: 11741828]
- [17]. Brockington M, Blake DJ, Prandini P, Brown SC, Torelli S, Benson MA, Ponting CP, Estournet B, Romero NB, Mercuri E, Voit T, Sewry CA, Guicheney P, Muntoni F. Mutations in the fukutin-related protein gene (FKRP) cause a form of congenital muscular dystrophy with secondary laminin alpha2 deficiency and abnormal glycosylation of alpha-dystroglycan. *Am. J. Hum. Genet.* 2001; 69:1198–1209. [PubMed: 11592034]
- [18]. Hu H, Li J, Gagen CS, Gray NW, Zhang Z, Qi Y, Zhang P. Conditional knockout of protein O-mannosyltransferase 2 reveals tissue specific roles of O-mannosyl glycosylation in brain development. *J. Comp Neurol.* 2011; 519:1320–1337. [PubMed: 21452199]
- [19]. Liu J, Zhang L, Wang D, Shen H, Jiang M, Mei P, Hayden PS, Sedor JR, Hu H. Congenital diaphragmatic hernia, kidney agenesis and cardiac defects associated with Slit3-deficiency in mice. *Mech. Dev.* 2003; 120:1059–1070. [PubMed: 14550534]
- [20]. Kano H, Kobayashi K, Herrmann R, Tachikawa M, Manya H, Nishino I, Nonaka I, Straub V, Talim B, Voit T, Topaloglu H, Endo T, Yoshikawa H, Toda T. Deficiency of alpha-dystroglycan in muscle-eye-brain disease. *Biochem. Biophys. Res. Commun.* 2002; 291:1283–1286. [PubMed: 11883957]
- [21]. Michele DE, Barresi R, Kanagawa M, Saito F, Cohn RD, Satz JS, Dollar J, Nishino I, Kelley RI, Somer H, Straub V, Mathews KD, Moore SA, Campbell KP. Post-translational disruption of dystroglycan-ligand interactions in congenital muscular dystrophies. *Nature.* 2002; 418:417–422. [PubMed: 12140558]

- [22]. Kim DS, Hayashi YK, Matsumoto H, Ogawa M, Noguchi S, Murakami N, Sakuta R, Mochizuki M, Michele DE, Campbell KP, Nonaka I, Nishino I. POMT1 mutation results in defective glycosylation and loss of laminin-binding activity in alpha-DG. *Neurology*. 2004; 62:1009–1011. [PubMed: 15037715]
- [23]. Liu J, Ball SL, Yang Y, Mei P, Zhang L, Shi H, Kaminski HJ, Lemmon VP, Hu H. A genetic model for muscle-eye-brain disease in mice lacking protein O-mannose beta1,2-N-acetylglucosaminyltransferase (POMGnT1). *Mech. Dev.* 2006; 123:228–240. [PubMed: 16458488]
- [24]. Grewal PK, Holzfeind PJ, Bittner RE, Hewitt JE. Mutant glycosyltransferase and altered glycosylation of alpha-dystroglycan in the myodystrophy mouse. *Nat. Genet.* 2001; 28:151–154. [PubMed: 11381262]
- [25]. Takeda S, Kondo M, Sasaki J, Kurahashi H, Kano H, Arai K, Misaki K, Fukui T, Kobayashi K, Tachikawa M, Imamura M, Nakamura Y, Shimizu T, Murakami T, Sunada Y, Fujikado T, Matsumura K, Terashima T, Toda T. Fukutin is required for maintenance of muscle integrity, cortical histogenesis and normal eye development. *Hum. Mol. Genet.* 2003; 12:1449–1459. [PubMed: 12783852]
- [26]. Montanaro F, Lindenbaum M, Carbonetto S. alpha-Dystroglycan is a laminin receptor involved in extracellular matrix assembly on myotubes and muscle cell viability. *J. Cell Biol.* 1999; 145:1325–1340. [PubMed: 10366602]
- [27]. Ervasti JM, Campbell KP. A role for the dystrophin-glycoprotein complex as a transmembrane linker between laminin and actin. *J. Cell Biol.* 1993; 122:809–823. [PubMed: 8349731]
- [28]. Yamada H, Shimizu T, Tanaka T, Campbell KP, Matsumura K. Dystroglycan is a binding protein of laminin and merosin in peripheral nerve. *FEBS Lett.* 1994; 352:49–53. [PubMed: 7925941]
- [29]. Gee SH, Blacher RW, Douville PJ, Provost PR, Yurchenco PD, Carbonetto S. Laminin-binding protein 120 from brain is closely related to the dystrophin-associated glycoprotein, dystroglycan, and binds with high affinity to the major heparin binding domain of laminin. *J. Biol. Chem.* 1993; 268:14972–14980. [PubMed: 8325873]
- [30]. Smalheiser NR, Kim E. Purification of cranin, a laminin binding membrane protein. Identity with dystroglycan and reassessment of its carbohydrate moieties. *J. Biol. Chem.* 1995; 270:15425–15433. [PubMed: 7797531]
- [31]. Gee SH, Montanaro F, Lindenbaum MH, Carbonetto S. Dystroglycan-alpha, a dystrophin-associated glycoprotein, is a functional agrin receptor. *Cell.* 1994; 77:675–686. [PubMed: 8205617]
- [32]. Yamada H, Denzer AJ, Hori H, Tanaka T, Anderson LV, Fujita S, Fukuta-Ohi H, Shimizu T, Ruegg MA, Matsumura K. Dystroglycan is a dual receptor for agrin and laminin-2 in Schwann cell membrane. *J. Biol. Chem.* 1996; 271:23418–23423. [PubMed: 8798547]
- [33]. Peng HB, Ali AA, Daggett DF, Rauvala H, Hassell JR, Smalheiser NR. The relationship between perlecan and dystroglycan and its implication in the formation of the neuromuscular junction. *Cell Adhes. Commun.* 1998; 5:475–489. [PubMed: 9791728]
- [34]. Talts JF, Andac Z, Gohring W, Brancaccio A, Timpl R. Binding of the G domains of laminin alpha1 and alpha2 chains and perlecan to heparin, sulfatides, alpha-dystroglycan and several extracellular matrix proteins. *EMBO J.* 1999; 18:863–870. [PubMed: 10022829]
- [35]. Sato S, Omori Y, Katoh K, Kondo M, Kanagawa M, Miyata K, Funabiki K, Koyasu T, Kajimura N, Miyoshi T, Sawai H, Kobayashi K, Tani A, Toda T, Usukura J, Tano Y, Fujikado T, Furukawa T. Pikachurin, a dystroglycan ligand, is essential for photoreceptor ribbon synapse formation. *Nat. Neurosci.* 2008; 11:923–931. [PubMed: 18641643]
- [36]. Hu H, Yang Y, Eade A, Xiong Y, Qi Y. Breaches of the Pial Basement Membrane and Disappearance of the Glia Limitans during Development Underlie the Cortical Lamination Defect in the Mouse Model of Muscle-eye-brain Disease. *J. Comp Neurol.* 2007; 501:168–183. [PubMed: 17206611]
- [37]. Yang Y, Zhang P, Xiong Y, Li X, Qi Y, Hu H. Ectopia of meningeal fibroblasts and reactive gliosis in the cerebral cortex of the mouse model of muscle-eye-brain disease. *J. Comp Neurol.* 2007; 505:459–477. [PubMed: 17924568]

**Highlights of this paper**

Three kinds of mouse models of congenital muscular dystrophies have been employed.

The similarities in morphology of different kinds of mouse models are impressive .

The disturbance of pial basement membrane and ectopia of granule cell precursors were observed.



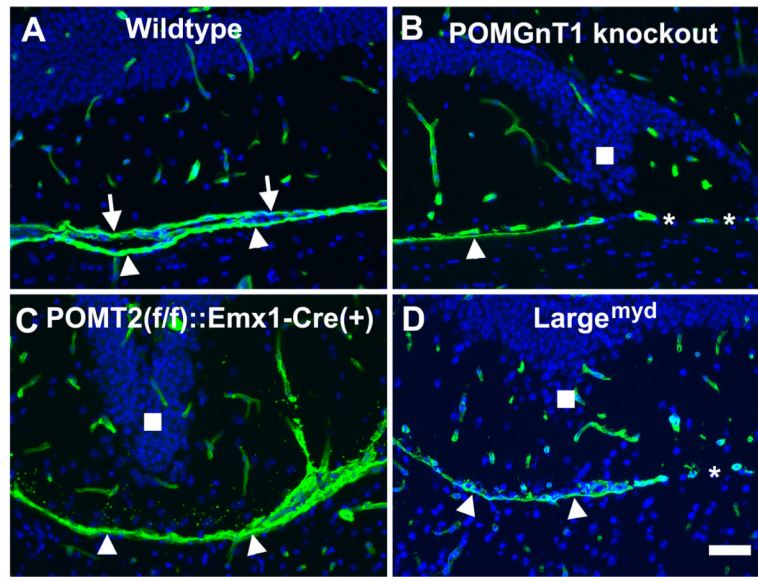


**Fig.1.**

Laminin immunofluorescence staining suggests disruption of the pial basement membrane in the dentate gyrus of CMD mouse models.

Coronal sections of adult forebrain were immunostained with anti-laminin (green fluorescence) and counterstained with DAPI (blue fluorescence). (A) Wild type. Laminin immunofluorescence was observed in blood vessels and pial basement membrane. The pial basement membrane of the dentate gyrus (arrows) and the midbrain (arrowheads) were clearly discerned. (B) POMGnT1 knockout. In some regions only a single pial basement membrane, presumably of the midbrain, was observed (arrowhead). There were regions devoid of any pial basement membrane separating the dentate gyrus and the midbrain (asterisks). (C) POMT2<sup>f/f</sup>;Emx1-Cre(+). A single pial basement membrane is observed between the dentate gyrus and the midbrain (arrowheads). (D) Large<sup>myd</sup> mice. Regions of single pial basement membrane (arrowheads) and regions with no pial basement membrane were observed. Scale bar in D: 50 μm.

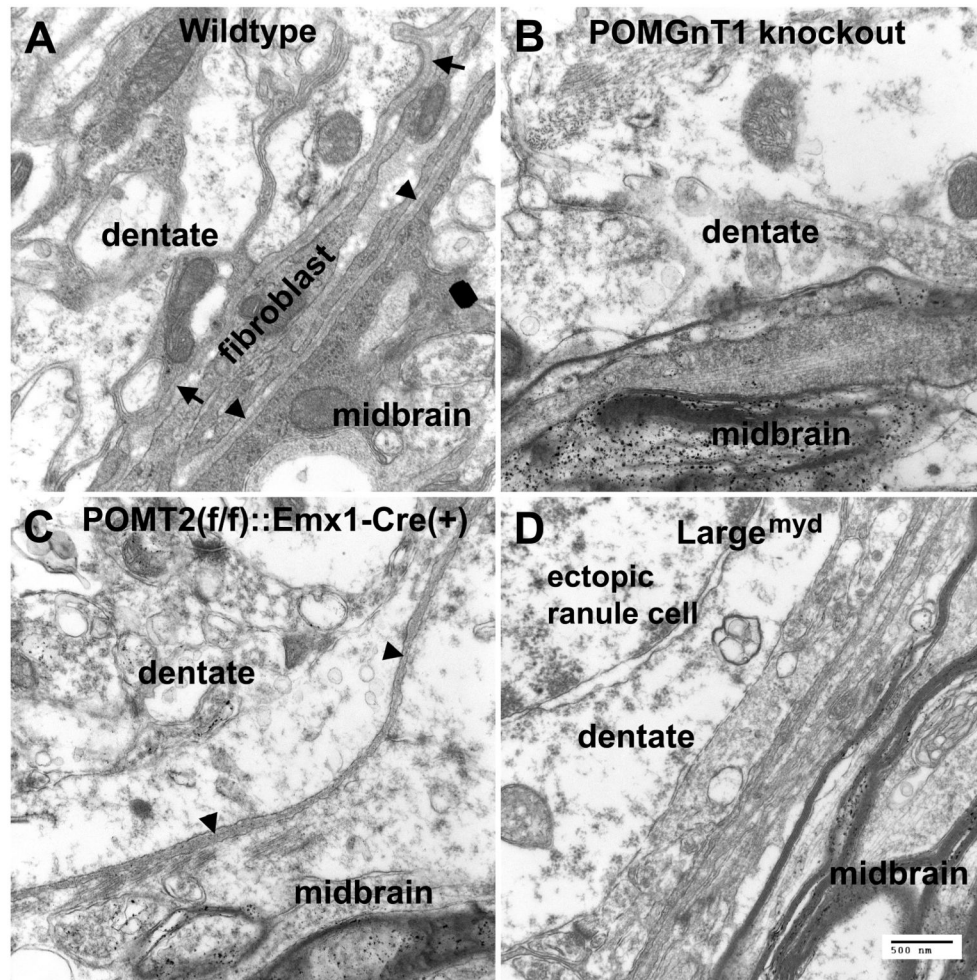


**Fig.2.** EM analysis confirmed pial basement membrane disruptions at the dentate gyrus. Adult dentate gyrus was fixed with 3.7% glutaraldehyde and processed for transmission EM analysis. (A) Wildtype. The pial basement membrane of the dentate gyrus (arrows) and the midbrain (arrowheads) was clearly distinguished. Both pial basement membranes were separated by fibroblasts. (B) POMGnT1 knockout. In this example, no pial basement membrane was observed between the dentate gyrus and the midbrain. (C) POMT2<sup>f/f</sup>::Emx1-Cre(+). A single pial basement membrane belonging to the midbrain (arrowheads) was identified. (D) Large<sup>myd</sup> mice. No pial basement membrane was seen between the dentate gyrus and the midbrain. An ectopic granule cell appeared on this section. Scale bar in D: 500 nm.

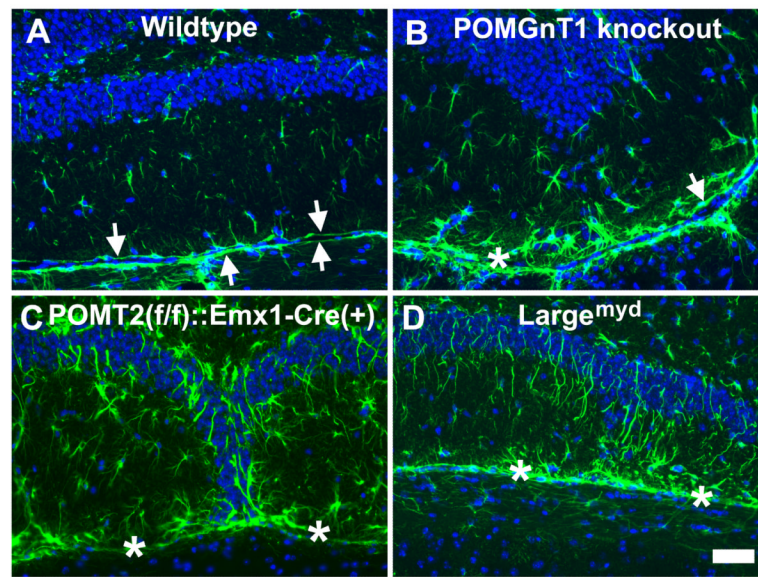


**Fig.3.**

Reactive astrogliosis was present at the dentate gyrus of the knockout animals. Coronal sections of adult brain were immunofluorescence stained with anti-GFAP (green fluorescence) and counterstained with DAPI counter staining (blue fluorescence). (A) Wildtype. GFAP immunofluorescence was observed at two continuous glia limitans separating the dentate gyrus and the midbrain (arrows). GFAP-positive astrocytes were sporadically positioned within the lower blade of the dentate. (B) POMGnT1 knockout. Glia limitans were observed (arrow) but discontinuous (asterisk indicates breaks). GFAP-positive astrocytes with increased size were frequently observed within the lower blade. (C) POMT2<sup>f/f</sup>;Emx1-Cre(+). Breaks in glia limitans (asterisks) were frequently observed. GFAP-positive astrocytes were increased over the wildtype. (D) Large<sup>myd</sup> mice. Breaks in glia limitans were observed (asterisks) and increased GFAP-immunofluorescence was apparent. Scale bar in D: 50  $\mu$ m.

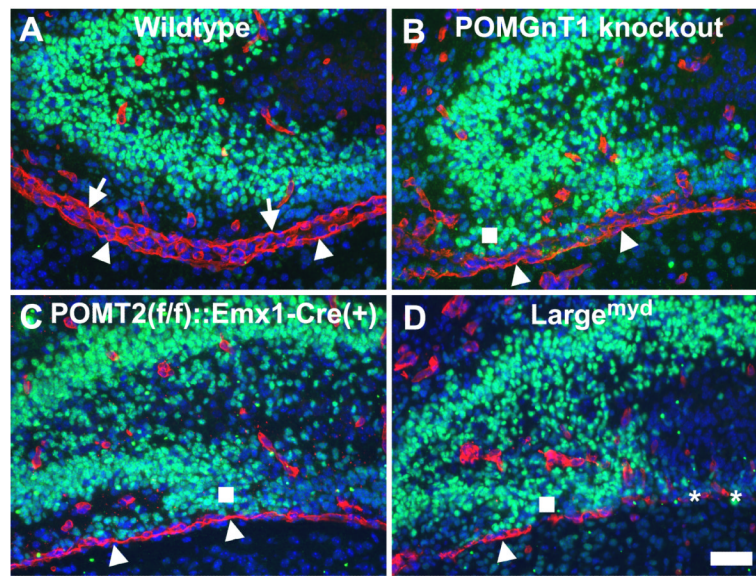


**Fig.4.**

Breaches in the pial basement membrane causes ectopia of granule cell precursors during development.

Newborn forebrain sections were double stained with antibodies against laminin-1 (red fluorescence) and Prox1 (green fluorescence) and counterstained with DAPI (blue fluorescence). (A) Wildtype. The pial basement membrane of the dentate gyrus (arrows) and the midbrain (arrowheads) was clearly observed. Prox1-positive granule cells in the lower blade were separated from the pial basement membrane by at least 50  $\mu\text{m}$ . (B) POMGnT1 knockout. The pial basement membrane of the dentate gyrus in this section was broken into pieces while the pial basement membrane of the midbrain appeared intact. Ectopia of Prox1-positive granule cells was apparent (square). (C) POMT2<sup>f/f</sup>;Emx1-Cre(+). The pial basement membrane of the dentate gyrus was absent in this section while the pial basement membrane of the midbrain was intact. Ectopic Prox1-positive granule cells were clearly observed (square). (D) Large<sup>myd</sup> mice. In this section, the pial basement membrane of the dentate gyrus was absent and the pial basement membrane of the midbrain was also disrupted. Where indicated by asterisks, there was no intact pial basement membrane. Ectopia of Prox1-positive neurons was clearly observed. Scale bar in D: 50  $\mu\text{m}$ .